

Estimates of Atmosphere-Induced Gain Loss for the Deep Space Network Array

L. R. D'Addario¹

Decorrelation of carrier phases among the antennas of the Deep Space Network (DSN) Array may occur due to turbulence in the Earth's atmosphere, leading to a reduction in signal-to-noise ratio for both received and transmitted signals if no correction is made. In this article, available statistical data on the turbulence are collected and analyzed in an attempt to predict the magnitude of such a loss.

I. Background

The current concept for the future of the Deep Space Network (DSN) includes large arrays of small paraboloidal reflector antennas [1]. About 400 antennas of 12-m diameter are planned at each of three longitudes. Their arrangement on the ground is a trade-off between avoiding shadowing at low elevations (favoring a wide distribution) and minimizing the decorrelation and loss of gain caused by variation in the delay through the troposphere from one antenna to another (favoring a maximally compact distribution). Secondary considerations include minimizing side lobes in the array beam and minimizing cost. All of this has been discussed in [2] by D. Jones, leading to a proposed antenna distribution that extends across about 1.6 km. That distribution is plotted in Fig. 1. In it the minimum spacing between antennas is 45 m, and the maximum is 1751 m.

Shadowing for the proposed array is well quantified [2], with the fraction of antennas having any amount of shadowing ranging from 19 percent at 10-deg elevation (worst azimuth) to 5 percent at 20 deg. The atmospheric decorrelation is less well established, largely because it is a statistical quantity that is site-dependent. Estimates were made by D. Bagri [3] using water vapor radiometer data from Goldstone, but that method is very indirect and uncertain. Direct observations of the microwave turbulence are possible using a small interferometer observing a geostationary satellite with a baseline of several hundred meters. Such systems have been in operation for many years at several radio astronomy sites, but not at the present or future DSN sites. Still more direct information can be extracted from the calibration observations regularly carried out by operational synthesis telescopes like the Very Large Array (VLA), the Australia Telescope, and the Berkeley-Illinois-Maryland Array (BIMA) millimeter array; this provides data on a wider range of baselines than the test interferometers that use satellites (which typically have only one baseline), but usually the integrating times are longer than desired for good measurements of the turbulence. A few studies using specially collected measurements from such telescopes allow more detailed analysis [4,10-12].

¹ Tracking Systems and Applications Section.

The research described in this publication was carried out by the Jet Propulsion Laboratory, California Institute of Technology, under a contract with the National Aeronautics and Space Administration.

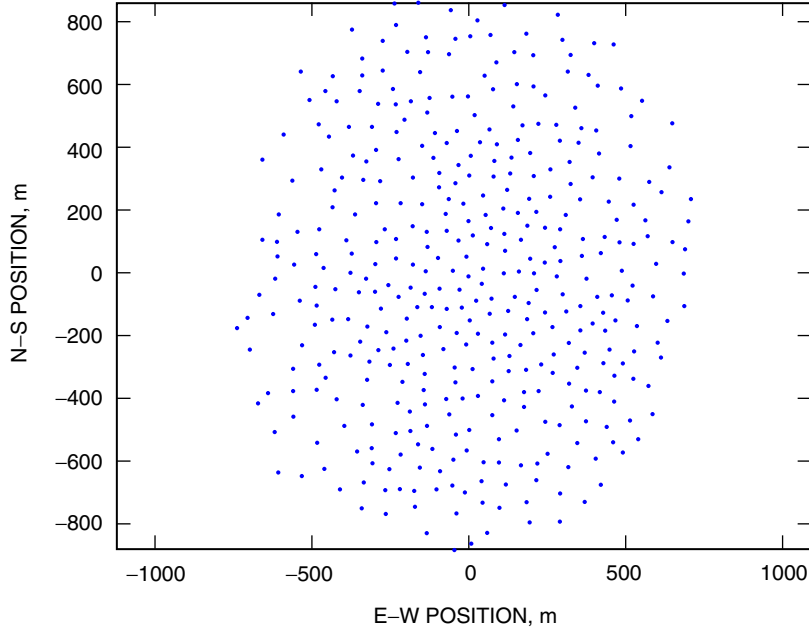


Fig. 1. Configuration of 400 antenna elements proposed for the DSN Array in [2].

In this article, I attempt to collect some of the available data on atmospheric turbulence and apply it to the specific configuration proposed for the DSN Array. The result is a prediction of the loss in gain that will occur if no correction for the turbulence is made but the array is otherwise accurately aligned. The analysis is based on transmitting (uplink direction), but the same loss of gain (or effective collecting area) occurs when receiving.

II. Summary of Available Measurements

The excess path delay through the atmosphere is conveniently characterized by its statistical *structure function*, defined by

$$D(r) = \left\langle [\tau(\vec{x}) - \tau(\vec{x} - \vec{r})]^2 \right\rangle \quad (1)$$

where $\tau(\vec{x})$ is the delay above geographic position \vec{x} on the Earth's surface. It is thus assumed that the distribution is spatially stationary, so that it depends only on the difference between positions; we further assume that it depends only on the magnitude of that difference, $r = |\vec{r}|$, even though a direction dependence could be introduced by wind. There is both theoretical and experimental evidence that $D(r)$ is well approximated by a power law function of the form

$$D(r) = D(r_0) \left(\frac{r}{r_0} \right)^\beta \quad (2)$$

Kolmogorov turbulence theory predicts this form with $\beta = 5/3$ for $r \ll h$, where h is the thickness of the turbulent air layer, and $\beta = 2/3$ for $r \gg h$ [7]. Direct measurements of $D(r)$ are possible from radio source observations with an array that provides a range of antenna spacings simultaneously. Such studies have been done at the VLA [10,11] at 22 GHz and at the BIMA telescope [12] at 86 GHz. Indirect

measurements are possible with a single interferometer by rapidly recording a time series of visibility phase delay measurements and computing the temporal structure function,

$$D_t(T) = \left\langle [\tau(t) - \tau(t - T)]^2 \right\rangle$$

By assuming that the turbulence remains “frozen” for a significant time and is carried across the interferometer by the wind, we can estimate that $D(r) \approx D_t(b/v - r/v)$, where b is the spacing (baseline) of the interferometer and v is the component of wind velocity along the baseline, for $r < b$. It is usually observed that $D_t(T)$ increases with T up to some interval T_b , after which it is flat; this provides an estimate of the wind speed as $v = b/T_b$. In this way, it is possible to fit the measurements to the model in Eq. (2) so as to derive values of $D(r_0)$ and β , and then to use the model to extrapolate $D(r)$ to a wider range of r .

Single-baseline test interferometers have been set up at various sites around the world for the purpose of determining the turbulence-induced delay statistics at those sites. These instruments have usually used small antennas observing a geostationary satellite, and in some cases data have been collected over several years. They have used baselines of $b = 50$ to 300 m.

Measurements from several of these site-test interferometers are summarized in Table 1. The long-term rms delay difference $\sqrt{D(r)}$ at $r = 300$ m in the zenith direction is given for each case. The reported results have been converted, if necessary, from phase at the measurement frequency to delay, from the measurement elevation to zenith, and from the measurement baseline to 300 m using Eq. (2) with $\beta = 1.3$. However, each site has substantial day/night and seasonal variation, so the median for one observing session or tracking pass could be substantially worse than the long-term value.

Fittings to Eq. (2) using these single-baseline measurements give β between 1.2 and 1.5, somewhat below the thick-layer value (5/3) and above the thin-layer value (2/3) of the theory, suggesting a variable-thickness layer or a two-layer structure [8] for $r < 300$ m. On the other hand, the VLA multi-baseline data [10,11] give $\beta = 0.58$ to 0.84 (but with wide day-to-day variation), near the thin-layer value, but most of the data are at $r > 1$ km. Evidence in [12] suggests that the frozen-pattern hypothesis may not hold, so that the single-baseline data cannot be reliably used to estimate β .

A more thorough discussion and a review of measurements prior to 1996 are given in [12].

Table 1. Site test interferometer data.

Reference	Location	Elevation, m	Measurement frequency, GHz	Baseline, m	Duration	Long-term rms, ^a ps
[4]	VLA	2100	11.3	300	1 year	1.70
[5]	LMT site ^b	4600	11.7	50	28 days	0.80
[6]	ALMA site	5000	11.7	300	7 years	0.79
[9]	Mauna Kea	4069	11.7	100	8 years	0.57

^a Median (50th percentile) of $\sqrt{D(300\text{ m})}$ derived from many separate time series, each 5 min to 60 min long.

^b The Large Millimeter Telescope.

Overall, the evidence favors a model with $\beta \approx 1.6$ for short baselines and $\beta \approx 0.7$ for long baselines, where both the overall scale and the crossover baseline length vary with site, season, time of day, and weather. Of the published data, only the VLA and the Atacama Large Millimeter Array (ALMA) measurements are available as a function of time of year and day and also as cumulative distributions, but most of these data are from the single-baseline test interferometers. In the remainder of this article, the turbulence is characterized by the single parameter $D(300\text{ m})$, which is taken to have a probability distribution that varies with time and site. The structure function at other baseline lengths is extrapolated as a power law using the fixed exponents just given, and with a fixed crossover baseline of 0.5 km. The statistics of $D(300\text{ m})$ are taken primarily from the VLA data. Adjustments for elevation angle e are made by assuming that $D(r)$ scales with air mass $1/\sin e$.

III. Theory

The complex amplitude of the far-field pattern of a phased array may be written

$$V = \sum_k A_k e^{-j2\pi\tau_k f} \quad (3)$$

where $A_k = a_k e^{j\phi_k}$ is the complex amplitude of the wavefront at element k , τ_k is the propagation delay from that element to the far-field point, and f is the frequency. For our purposes, this can be simplified by assuming that all wavefront amplitudes are the same, $a_k = a$, and that ϕ_k is automatically adjusted to track $2\pi\tau_k f$ as closely as possible according to a geometrical model. If the tracking is perfect, we find $V = Na$, where N is the number of elements. But the tracking will not be perfect, partly because the turbulence in the atmosphere causes unmodeled fluctuations in τ_k , and that is what we wish to investigate. Let $\theta_k = \phi_k - 2\pi\tau_k f$ be the phase tracking error, and assume that it is due entirely to the atmospheric turbulence. Then

$$V = a \sum_k e^{j\theta_k} \quad (4)$$

We treat θ_k statistically. The expected value of the flux density (power) at the far-field point is then

$$\begin{aligned} \langle |V|^2 \rangle &= a^2 \left\langle \left| \sum_k e^{j\theta_k} \right|^2 \right\rangle \\ &= a^2 \left\langle \left| \sum_k \cos \theta_k + j \sin \theta_k \right|^2 \right\rangle \\ &= a^2 \left\langle \left(\sum_k \cos \theta_k \right)^2 + \left(\sum_k \sin \theta_k \right)^2 \right\rangle \\ &= a^2 \sum_k \sum_m \langle \cos \theta_k \cos \theta_m + \sin \theta_k \sin \theta_m \rangle \\ &= a^2 \sum_k \sum_m \langle \cos(\theta_k - \theta_m) \rangle \end{aligned} \quad (5)$$

Thus, the expected power (and, more generally, all statistics of the far-field power) depends only on the statistics of the phase *differences* among all antenna pairs of the array. Finally, we use the general theorem that if x is any zero-mean, normally distributed random variable, then $\langle \cos x \rangle = e^{-\sigma_x^2/2}$, where $\sigma_x^2 = \langle x^2 \rangle$. This gives

$$\begin{aligned} \langle |V|^2 \rangle &= a^2 \sum_k \sum_m \exp [-\langle (\theta_k - \theta_m)^2 \rangle] \\ &= a^2 \sum_k \sum_m \exp [-(2\pi f)^2 D(r_{km})] \end{aligned} \quad (6)$$

where r_{km} is the distance between elements k and m . We have thus assumed that the phase differences are all zero mean and normally distributed. Note that this analysis is exact, in that it does not involve any mathematical approximations such as small phase angles.

IV. Results

Equation (6) has been evaluated for the proposed antenna arrangement of Fig. 1 using the phase stability statistics measured at the VLA [4], and using

$$D(r) = \begin{cases} D(500 \text{ m})(r/500 \text{ m})^{1.6}, & r \leq 500 \text{ m} \\ D(500 \text{ m})(r/500 \text{ m})^{0.7}, & r > 500 \text{ m} \end{cases} \quad (7)$$

A histogram of the distribution of antenna spacings is plotted in Fig. 2. As shown in Table 1, the long-term zenith rms delay at the VLA is about 1.7 ps, but the data in [4] are analyzed into 24 separate bins, representing the daytime and nighttime results for each of the 12 calendar months. Within each bin, the cumulative distribution of 10 minute averages is calculated, so we have not only the median but all percentiles. Here we choose to examine only the 90th percentile conditions (where the decorrelation is equal or better 90 percent of the time). The best bin is then nighttime in December, where the value is 1.23 ps; the worst is daytime in September, 6.98 ps. In the same month, daytime values are typically about twice the nighttime ones at all percentiles.

Figure 3 shows the calculated overall decorrelation for the array as a function of frequency, for the best and worst VLA bins and at elevations of 90 deg and 20 deg, all at the 90th percentile. It can be seen that for cold nights the loss is less than 8 percent at 34 GHz, even at 20-deg elevation. But for warm days we see about 68 percent loss (−4.9 dB) at zenith and 83 percent (−7.7 dB) at 20 deg. However, at 8 GHz the loss remains less than 16% (−0.75 dB) in all cases (at the 90th percentile).

V. Conclusion

The VLA site has a desert climate and is at about 2100 m above sea level. If it can be taken as representative of future DSN sites, then arrays of the intended size (about 1.6 km across) can expect very little decorrelation when operating in the 7.1- to 8.5-GHz band. It appears that the decorrelation at 20-deg elevation will be less than 1 dB at least 99 percent of the time. On the other hand, operation in the 26- to 41-GHz range is expected to incur far higher loss during summer daytime conditions if no correction is made. To ensure adequate availability, active real-time phase corrections should be implemented at the higher frequencies, but they are probably unnecessary at the lower frequencies.

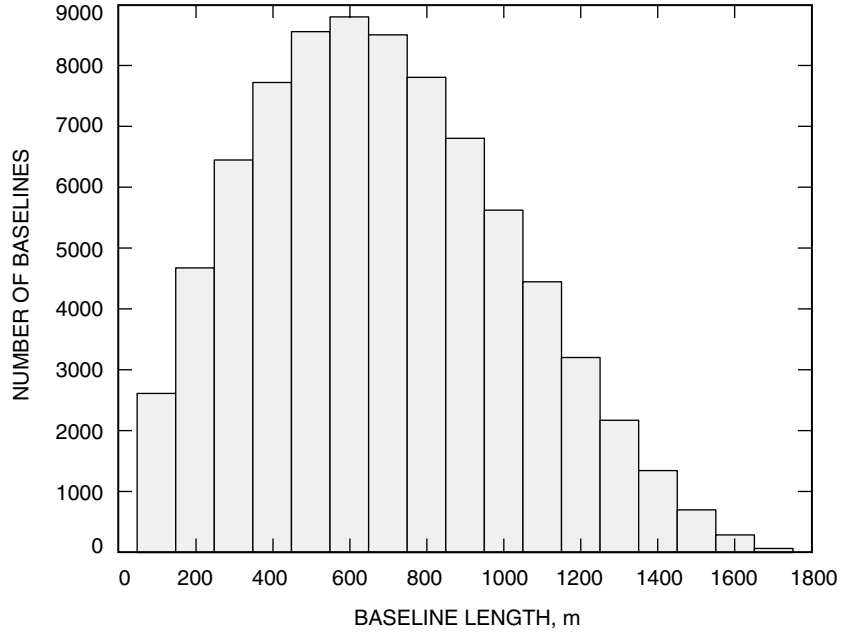


Fig. 2. Histogram of antenna spacings for the proposed array of Fig. 1.

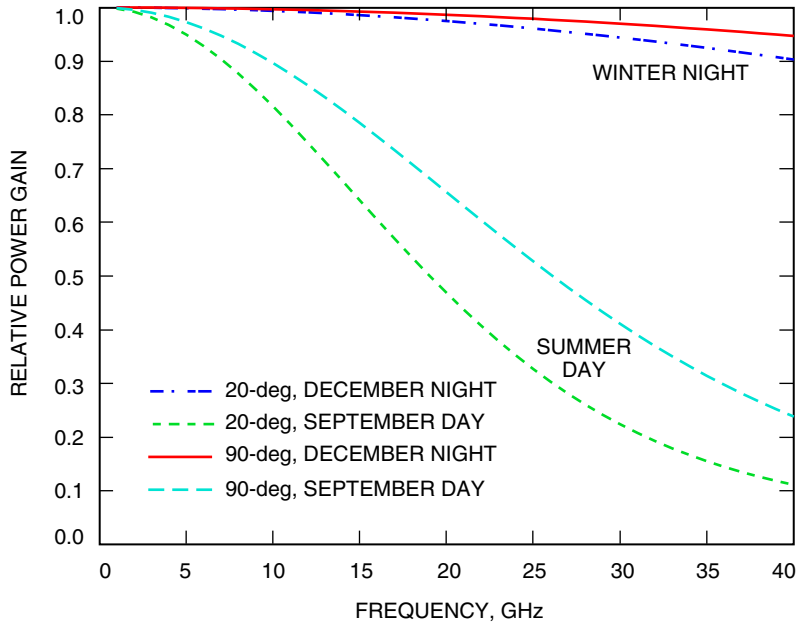


Fig. 3. Relative gain due to atmospheric path delay fluctuation (coherence loss) at zenith and 20-deg elevation for the best and worst months at the VLA, under 90th percentile conditions (i.e., the gain is predicted to be greater than the indicated value 90 percent of the time during the given half-month).

References

- [1] *The Interplanetary Network Progress Report, Special Issue on Array Developments in the Deep Space Network*, vol. 42-157, Jet Propulsion Laboratory, Pasadena, California, May 15, 2004.
http://ipnpr/progress_report/42-157/title.htm
- [2] D. L. Jones, "Geometric Configuration Constraints for Large Deep Space Network Arrays," *The Interplanetary Network Progress Report*, vol. 42-157, Pasadena, California, pp. 1–9, May 15, 2004.
http://ipnpr/progress_report/42-157/157F.pdf
(Later updated: D. Jones, "Antenna Separations and Configurations for DSN Arrays," Memorandum to J. Statman et al. (internal document), Jet Propulsion Laboratory, Pasadena, California, November 9, 2004.)
- [3] D. S. Bagri, "The Effect of Atmospheric Phase Fluctuations on Uplink Arraying," *The Interplanetary Network Progress Report*, vol. 42-157, Jet Propulsion Laboratory, Pasadena, California, pp. 1–7, May 15, 2004.
http://ipnpr/progress_report/42-157/157K.pdf
- [4] B. Butler and K. Desai, "Phase Fluctuations at the VLA Derived from One Year of Site Testing Interferometer Data," VLA Test Memorandum 222, National Radio Astronomy Observatory, October 1, 1999.
- [5] D. Hiriart and J. Valdez, "Radio Seeing Monitor Interferometer," *Pub. Astron. Soc. Pac.*, vol. 114, pp. 1150–1155, 2002.
- [6] S. Radford, data available at
<http://www.tuc.nrao.edu/mma/site/Chajnantor/data.c.html>
- [7] C. Coulman, "Fundamental and Applied Aspects of Astronomical Seeing," *Ann. Rev. Astron. Astrophys.*, vol. 23, pp. 19–57, 1985.
- [8] C. Carilli and M. Holdaway, "Tropospheric Phase Calibration in Millimeter Astronomy," *Radio Science*, vol. 34, pp. 817–840, 1999.
- [9] D. Wilner, "The Submillimeter Array and FIRST/Herschel," FIRST Workshop of 2001-02-13, available at
http://cfa-harvard.edu/~dwilner/smasci/talk_resources/first01
- [10] R. Sramek, "Atmospheric Phase Stability at the VLA," URSI/IAU Symposium on Radio Astronomical Seeing, Beijing, China, May 1989; available as VLA Test Memorandum 175, National Radio Astronomy Observatory, September 1993.
- [11] C. L. Carilli and M. Holdaway, "Application of Fast Switching Phase Calibration at mm Wavelengths on 33 km Baselines," MMA Memorandum 173, National Radio Astronomy Observatory, May 22, 1997; quoted in [10].
- [12] M. Wright, "Atmospheric Phase Noise and Aperture-Synthesis Imaging at Millimeter Wavelengths," *Pub. Astron. Soc. Pac.*, vol. 108, pp. 520–534, June 1996.